A comparison of azimuthal and axial oscillation microfiltration using surface and matrix types of microfilters with a cake-slurry shear plane exhibiting non-Newtonian behaviour

Journal of Membrane Science 550 (2018) 357–364

Contents lists available at ScienceDirect

Journal of Membrane Science

journal homepage: www.elsevier.com/locate/memsci

A comparison of azimuthal and axial oscillation microfiltration using surface and matrix types of microfilters with a cake-slurry shear plane exhibiting non-Newtonian behaviour

Richard Holdich[a,*], Keith Schou[a], Marijana Dragosavac[a], Simon Kellet[b], Hemaka Bandulasena[a]

[a] Chemical Engineering Department, Loughborough University, Leics. LE11 3TU, UK
[b] Sellafield Ltd., Seascale, Cumbria CA20 1PG, UK

ARTICLE INFO

Keywords:
Shear stress
Modelling
Non-Newtonian
Membrane fouling
Calcite

ABSTRACT

The mode of application of oscillation, axial or azimuthal, did not influence filtration performance, when filtering a calcite mineral with a d_{32} value of 2.7 μm. The equilibrium flux and deposit thickness correlated with shear stress, regardless of: filter type (metal slotted surface filter or homogeneous sintered filter); and mode of oscillation. Shear stress values up to 240 Pa were used and the particle compact believed to be at, or near, the deposited solids showed non-Newtonian flow behaviour described by the Herschel-Bulkley equation. The shear was computed using Comsol® to model the shear at, and near, the oscillating surface. The peak shear (maximum value) was used in the correlation for flux, which appeared to fit the data well and provide a realistic prediction for sustainable flux using a force balance model.

The existence of a yield stress in the compact appeared to limit the internal fouling of the matrix (homogeneous) type of filter, which had a membrane thickness of 8 mm, but did not demonstrate significant internal fouling over time, nor between filtrations. Thus, the results were similar to those obtained for the surface filters, and the resistance to filtration was dominated by the deposit formed.

1. Introduction

Microfiltration is used in a wide variety of process applications, and has had many years of academic investigation of factors influencing its operation and mathematical analysis of permeate flux [1]. Crossflow filtration is often applied due to its simplicity of design and operation. However, there are limitations in terms of the shear that can be obtained at the surface of the membrane, required to reduce the deposition of solids, and the inefficiency resulting from having to recycle the feed suspension over the membrane to provide economic operation. This recirculation, through what is often a high shear pump, can lead to the break-up of shear sensitive particles, e.g. flocs as well as sludge of a biological origin, generating finer particles which are more difficult to be filtered [2]. Hence, there has been increasing interest in Dynamic Filtration (DF), and enhanced shear microfiltration, where the shear at the membrane surface is not solely dependent on the crossflow rate, but is augmented by relative oscillation between the filter and slurry, or by rotation of the membrane, or surface close by [3].

There are a number of commercial, or semi-commercial, DF systems currently in use, or development [4]. The shear stress at the surface ranges from 0.35Pa to 39 Pa for these devices, when using the rheological properties of water to convert shear rate to stress. Oscillating azimuthal systems (VSEP, New Logic) are reported to show up to 17 times improvements in the permeate flux rate [3,4]. Rotating membrane discs (SpinTek) [5] have demonstrated dewatering from 5% to 15% during an endurance test of over 1500 h. Stationary membranes with rotating discs/impellers: DYNO; BOKELA; OPTIFILTER exist to enhance the shear at, or near to, the membrane surface. Other designs include: overlapping rotational membranes [6,7], overlapped counter-rotational membranes/impellers [8], helical rotating membranes [9–11], magnetically induced membrane vibrations [12], and axially oscillated hollow tube filters in membrane bio-reactors [13]. Filter designs that involve a moving membrane, or surface near to it, are more complex than simple crossflow systems, but they may provide a practical alternative to crossflow if they can sustain an appreciable flux and if they are less damaging to the material to be filtered. One potential application of such technology is in the nuclear industry, as part of reprocessing operations where the post-operational clean-out of reprocessing facilities, and the retrieval of waste from high-hazard "legacy" facilities, require the removal of particulate materials present at

* Corresponding author.
E-mail addresses: r.g.holdich@lboro.ac.uk (R. Holdich), K.Schou@Lboro.ac.uk (K. Schou), M.Dragosavac@lboro.ac.uk (M. Dragosavac), simon.kellet@sellafieldsites.com (S. Kellet), H.C.H.Bandulasena@lboro.ac.uk (H. Bandulasena).

https://doi.org/10.1016/j.memsci.2017.12.079
Received 27 July 2017; Received in revised form 2 November 2017; Accepted 29 December 2017
Available online 30 December 2017
0376-7388/

low concentrations in several effluent streams prior to conditioning (e.g. through encapsulation in cement) for long-term storage and disposal. For example at Sellafield, UK, iron oxyhydroxide flocs are precipitated by caustic dosing acid streams and then membrane filtered in order to remove transuranic species in the Enhanced Actinide Removal Process. Under these circumstances the ability to filter in a once-through (rather than recycled) system and, possibly, using a pump to suck the permeate through the membrane (avoiding pumping an abrasive suspension or one that breaks up within the pump) would be additional advantages, for example reducing the cost of providing containment and shielding and making the technology viable for small, mobile local effluent treatment plants.

Oscillations have been shown to have a greater effect on the shear at the surface of a filter than simple rotational systems [14,15], due to fluid inertia. There have been a number of academic studies of oscillating microfiltration [16,17]. In most cases the experimental approach has been to investigate Newtonian systems at low feed concentration. Many of these studies have used yeast suspensions [18] and algae [19], and reported the interaction of yeast fouling the membrane surface and pores. In most cases membrane blocking models have been developed [20]. Pulsatile flow at the surface of a membrane has been subjected to CFD analysis, but again due to the complexity of the problem this has been restricted to Newtonian systems [21]. It is the nature of fine colloidal suspensions that at the high solids content to be expected at, or near, the filter surface the rheological behaviour at the interface between the stationary membrane (or deposit) and the surrounding suspension will be non-Newtonian and may well exhibit a yield stress. This rheological behaviour will complicate the analysis of shear stress and application of microfiltration modelling.

The objectives of this study are to investigate a precipitated material filtering in different modes of oscillation (axial and azimuthal) on different structural types of filter (matrix and surface microfilters), and to model the non-Newtonian shear plane that will arise between the attached deposit on the filter and the surrounding feed suspension. The modelling should, therefore, be used to understand the correlation of shear stress and resulting permeate rates, from the application of a force balance. Different structural filter types could provide different fouled membrane performance.

2. Method and materials

2.1. Analysis of results

For the modelling of crossflow microfiltration a number of authors [17,22–25] have reported a linear correlation between equilibrium flux (J_e) and shear. In many cases the shear *rate* is used, which may be adequate for Newtonian and low concentration systems, but for more complex systems (where the location of the shear plane may be uncertain) the shear *stress* (τ), rationalised on the basis of a friction model approach, [1,26] is more appropriate as it is the drag force that removes particles from the surface of the filter:

$$J_e = K_1 x\tau + K_0 \tag{1}$$

where x is particle diameter is K_1 is dependent on the frictional forces and K_0 arises due to electrostatic repulsion and any other force that may act to keep the particles from forming a cake. Following a force balance approach it is possible [1] to investigate the frictional constant (K_1) further, leading to the following equation for flux, based on material and membrane properties:

$$\boldsymbol{J = \frac{\varphi^{2/5}}{\eta k_n \mu_w} x\tau} \tag{2}$$

where η is the frictional coefficient relating the normal and tangential forces, k_n is the constant in the Stokes drag equation and ψ is a dimensionless number [27] depending on the state of filtration. At the start of filtration:

$$\varphi = \frac{L_m}{R_m x^2} \tag{3}$$

where L_m is the membrane thickness and R_m is the membrane resistance, and after a cake has formed:

$$\varphi = \frac{k}{x^2} \tag{4}$$

where k is the permeability of the cake formed on the membrane surface. Permeability can be estimated by several expressions, a fundamental approach is that due to Happel and Brenner [28]:

$$k = \frac{\left(2 - 3C^{\frac{1}{3}} + 3C^{\frac{5}{3}} - 2C^2\right)}{\left(3 + 2C^{\frac{5}{3}}\right)} \frac{x^2}{12C} \tag{5}$$

where C is the solid concentration by volume of the cake formed on the membrane surface and x is a representative particle diameter within the filter cake. However, it is well known that cakes formed during microfiltration tend to contain finer particles than the initial feed distribution [1], due to the preferential shear removal of the larger particles. There is also evidence that even during conventional dead-end cake filtration the performance is dominated by the fine particles present, which can percolate and deposit at pore constrictions. Thus, it is recommended that for the purpose of filtration modelling of permeability the surface area to volume (Sauter mean) diameter is not necessarily used, instead the particle size corresponding to the 10%, or even 5%, on the cumulative mass undersize curve may be more representative [29].

In Eq. (2) the frictional coefficient relating the normal and tangential forces and the constant in the Stokes drag equation can be combined in to a single constant. The constant in the unmodified Stokes drag expression (Eq. (6)) has the value of 3, but this expression was derived for a single sphere in an infinite fluid. It is common to modify the Stokes drag expression to account for the influence of a wall, or other particles, on the drag experienced by the particle of interest. For the purpose of the modelling here it is proposed that the influence of the surrounding particles will have something in the order of increasing the drag by a factor of 100, compared to that predicted by Eq. (6), and in the absence of any knowledge of the friction coefficient a value of unity will be assumed. Hence, the combined constant (β) has a value of 300 for the product of: k_n and η. This value of the combined constants appears to be reasonable based on the above description, and will be shown to fit the experimental data.

$$F_d = 3\pi\mu x u_x \tag{6}$$

Eqs. (2) and (5) can be used to determine the shear stress required to avoid the deposition of particles on to the membrane surface. This was originally known as the critical flux concept, which later became 'sustainable' flux acknowledging the likelihood of some very limited, and remaining constant, fouling of the membrane [30]. The relation between the required shear stress and the sustainable flux (J_s) is [1]:

$$\tau > = \frac{\beta\mu}{x^{1/5}} \left(\frac{L_m}{R_m}\right)^{-2/5} J_s \tag{7}$$

During microfiltration the transmembrane pressure (ΔP) can be related to the flux in the usual way based on Darcy's Law:

$$\Delta P = \mu(R_m + R_c)J \tag{8}$$

where R_c is the cake resistance. It is possible to relate the membrane resistance to the permeability of the membrane (k_m) in the usual way:

$$R_m = \frac{L_m}{k_m} \tag{9}$$

For a homogeneous matrix type of membrane, i.e. one made of sintered, or randomly packed, material rather than a surface filter then the membrane permeability may be modelled as a packed bed. This can

be used to determine the 'equivalent pore size' of the filter by following the Kozeny approach to hydraulic mean diameter (d_H), whereby the pore channel size is equal to the volume open to flow divided by the surface area of the bed:

$$d_H = \frac{AL_m\varepsilon_m}{AL_m(1-\varepsilon_m)S_v} \tag{10}$$

where A is the membrane area, ε_m is the voidage of the membrane and S_v is the specific surface area per unit volume of the particles making up the membrane. The specific surface area per unit volume of the membrane is not required, as it can be related to the membrane permeability (using the Kozeny-Carman expression for permeability) and hence membrane resistance, to result in the following equation for equivalent pore channel diameter:

$$d_H = \sqrt{\frac{5L_m}{\epsilon_m R_m}} \tag{11}$$

where 5 is used as the value of the Kozeny coefficient. The specific surface area per unit volume is required for the calculation of the shear stress within the filter matrix (R). This is the shear stress supplied by the permeate on the solid surface of the filter due to permeate flow within the membrane, which can be modelled as a packed bed. A force balance between the solids and the fluid provides the well-known equation for shear stress in the packed bed [31]:

$$R = \frac{\epsilon_m}{S_v(1-\epsilon_m)}\frac{dP}{dL} \tag{12}$$

where dP/dL is the dynamic liquid pressure gradient, which can be determined from the Kozeny-Carman equation, for a given flux rate (superficial velocity):

$$\frac{dP}{dL} = \mu\left[\frac{5(1-\epsilon_m)^2 S_v^2}{\epsilon_m{}^3}\right]J \tag{13}$$

The successful application of Eq. (1), and others, requires the knowledge of the shear stress at the membrane (or deposit) interface with the surrounding suspension. In the experimental system described here the membrane is oscillating and the suspension is deemed to be stationary. There are some well-known expressions for the shear at the surface of vibrating surfaces, but these are relevant to Newtonian fluid mechanics. When forming a filter cake, which is assumed to be attached to the oscillating membrane surface, it is likely that the shear plane between that cake and the surrounding suspension will be at a much higher concentration than that of the surrounding, or feed, concentration. It will be assumed that this shear plane is at a concentration negligibly less than the measured cake concentration on the filter. At high solids concentrations it is common for slurries to exhibit a yield stress as well as shear thinning behaviour. This can be modelled by the Herschel-Bulkley equation:

$$\tau = K\gamma^n + \tau_o \tag{14}$$

where γ is the shear rate, τ_o is the yield stress and both K and n are constants. No simple analytical expression exists for the shear stress at an oscillating surface with this type of non-Newtonian fluid behaviour. Therefore, Computational Fluid Dynamics was used to determine the shear stress using the rheological model given by Eq. (14).

2.2. Numerical simulations for analysis of shear stress

Deformation at the surface of the filter cake deposit and the flow of adjacent bulk suspension (treated as a viscous homogeneous fluid) were simulated by solving the Navier–Stokes and continuity equations using the low Reynolds number k-epsilon turbulent model available within Comsol Multiphysics® version 5.2a. The deposit was assumed to have uniform constitutive properties throughout and its rheological properties were defined by modified Herschel-Bulkley equation [32]:

$$\eta(\dot\gamma) = K\dot\gamma^{n-1} + \frac{\tau_0}{\dot\gamma}(1-\exp(-\alpha\dot\gamma)) \tag{15}$$

where η is the shear dependent viscosity, $\dot\gamma$ is the shear rate, K is the flow consistency index, n is the flow behaviour index, τ_0 is the yield stress and α is the regularisation parameter. The exponential part of the equation that includes the regularisation parameter avoids the apparent viscosity becoming infinity, when the shear rate approaches zero. As the value of the regularisation parameter increases, Eq. (15) approaches the original Herschel-Bulkley model. The bulk suspension well-away from the deposited cake is dilute and the fluid is essentially Newtonian with a constant viscosity. The particle concentration of the fluid in the vicinity of the filter cake surface drops sharply within a short radial distance; hence the rheological model parameters within this buffer region are varied exponentially as follows:

$$K(r) = K^*\exp(-5^*(r-(R+L))) + \mu_B$$

$$n(r) = (1-n)^*-\exp(-5^*(r-(R+L))) + 1$$

$$\tau_0(r) = \tau_0{}^*\exp(-5^*(r-(R+L)))$$

where r, R, L, μ_B are radial distance from the axis, filter radius, cake thickness and bulk viscosity of the suspension respectively. Using these spatially varying model constants, the local viscosity for the buffer region can be defined as,

$$\eta(\dot\gamma,\ r) = K(r)\dot\gamma^{n(r)-1} + \frac{\tau_0(r)}{\dot\gamma}(1-\exp(-\alpha\dot\gamma))$$

The density of the suspension in the buffer region is defined as,

$$\rho(r) = \rho_s + (\rho_c - \rho_s)^*\exp(-5^*(r-(R+L))$$

where ρ_s is the density of the bulk suspension and ρ_c is the density of the filter cake deposit.

The computational domain consists of a mid-section from the cylindrical filter and the end effects from the top and the bottom of the filter were neglected to simplify the problem. A case where 1.5 mm filter cake deposited on the filter surface is considered for the simulations. The problem was solved in a 2-D axisymmetric computational domain with a high mesh density near the cake surface to fully resolve the flow within the buffer region. The boundary condition at the filter surface and the outer vessel wall were set as azimuthal velocity with a sinusoidal variation and no-slip condition, respectively. The top and the bottom computational domain boundaries were set as slip boundaries. The filter cake and the bulk suspension including the buffer region were at rest initially and computations were carried out for five consecutive oscillation cycles. The low Re k-ε model used in this computational study resolves the flow all the way to the boundaries avoiding the use of wall functions; hence the fluid stresses at the cake surface can be calculated accurately. The problem was initially solved for a regularisation parameter of 1, and subsequently increased to 10 in several steps using the previous solution as the next initial condition to assist convergence. Mesh-independent solutions were obtained with 14 000 quadrilateral mesh elements, and confirmed using a higher mesh density of 28 000 elements. The total simulation time was approximately 3.5 h, on an Intel Core i7 64-bit 2.7 GHz processor, to establish the maximum shear stress condition for each of the frequencies and filter radii used. An example set of: displacement from the origin; fluid velocity and resulting shear stress all with respect to time over three cycles of oscillation, from the CFD analysis, is provided in the supplementary information (supplementary information 1 cfd example.csv) for one of the filtration conditions used.

2.3. Experimental

A batch filtration system was used, Fig. 1, where a suspension of calcite was stirred on a magnetic stirrer positioned 55 mm below the lowest point of the filter and rotating at 1 revolution per second. This

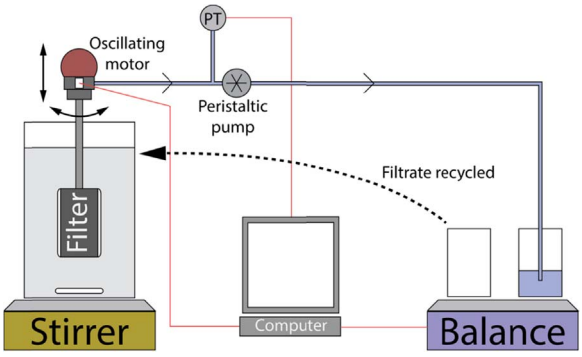

Fig. 1. Schematic illustration of oscillating filter experimental equipment.

was determined to be sufficient to maintain a uniform suspension. Permeate was sucked through a cylindrical filter using a peristaltic pump (Watson Marlow D401 UK). The experiments were conducted at room temperature 22 °C plus or minus 2 °C, there was no significant generation of heat during the runs. The pressure was measured using a Freescale Semiconductor MPX5700 pressure sensor connected to a 16 bit Adafruit Industries 4-Channel ADC Breakouts (ADS1115) sampling at 30 Hz connected to a PC via a Gravitech Arduino Nano (ATmega328) to give the transmembrane pressure. The mass of permeate (water) was logged against time to give the mass flow rate using a Sourcingmap Load Cell (US-SA-AJD-343700) connected to a Avia Semiconductor 24-Bit Analog-to-Digital Converter (HX711) and interfaced to a PC via another Arduino Nano. The sample frequency used was 12.5 Hz for both pressure and mass. Two modes of oscillation were investigated: axial and azimuthal. In the former case the axial oscillation was delivered by a Ling Dynamics System V500 oscillator powered by a PA100 amplifier. The oscillation signal was generated by a National Instruments digital to analog converter, controlled by a LabVIEW program running on a PC. Frequency and amplitude could be controlled independently, within the range possible from the PA100 amplifier (20–100 Hz). In the case of the azimuthal oscillation a much cheaper and simpler drive system was employed (Wilko Multi-Tool device obtained from a local hardware store), which uses a mechanically connected system of fixed oscillation angle (3 degrees), but variable frequency depending on the power supplied to the electric motor (20–100 Hz). For both types of oscillation the frequency and amplitude of the oscillation were measured, and logged to PC, using an accelerometer (Analog Devices ADXL335) and a Gravitech Arduino Nano (ATmega328) on-board ADC. In total three Arduinos were used, one for each sensor, to maximise signal processing speed from each sensor.

Three types of filter were tested, see Fig. 2: a nickel metal slotted filter (supplied by Micropore Technologies Wilton UK), an identical filter but with a PTFE coating on the surface, and a ceramic Coralith C0

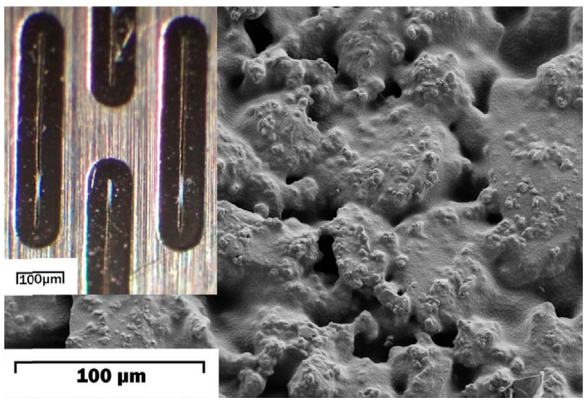

Fig. 2. Scanning Electron Microscope image of the filtering surface of the ceramic filter and top left inset showing slotted pore nickel filter.

grade microfilter (supplied by Mantec Stoke-on-Trent UK). Both types of nickel (and PTFE coated) filters were cylinders with 14 mm outside diameter, 64 mm membrane working length, 10 micrometre slot width and 400 micrometre slot length, with 300 micrometre membrane thickness (open area of filter pores 5%). These filters are surface filters, having pores that go straight through from one side of the membrane to the other, i.e. without a tortuous pore flow channel and no connection between the slotted pores. This membrane structure is very different to the more conventional ceramic microfilter tested, which had an outside diameter of 29 mm and working length 57 mm. The inside diameter of the ceramic filter, where the permeate was sucked in to, was 13 mm. Thus the membrane thickness was substantial at 8 mm. The filter was homogeneous, without any coating on the filtering surface, which was the outside of the filter tube. The SEM shown in Fig. 2 shows that the pore openings are around 10 micrometres in size, similar to the slot width of the metal/PTFE coated filter. The manufacturer data on the filter is supplied in Table 1. The porosity of the filter was measured by mass uptake of RO water, followed by drying, and was determined to be 37% void fraction. The material constituting the filter was checked using the Energy Dispersive X-Ray Spectrometer tool on an SEM. The results showed that the filter was 20% silica (SiO_2) and 80% alumina (Al_2O_3). Both of these minerals are highly hydrophilic with very low water contact angles, facilitating the wetting of this inorganic microfilter with water.

Permeate mass was measured using the balance and recorded on the PC, with periodic return of the permeate (up to 100 mL) back to the feed tank, which had an internal diameter of 125 mm and 2 l capacity. Permeate flux rate was determined by numerically differentiating the permeate mass curve with respect to time. The microfiltrations were run under conditions of constant rate at the start of the filtration, using a peristaltic pump, but with time the pressure and flow curves would stabilise at constant values as the pump reached the limit of pressure (i.e. suction) that it could deliver. The main objective was to investigate the equilibrium conditions, and their dependency on filter type and method of application and magnitude of shear. In general, this stabilisation occurred well within one hour of filtration. All results reported here have reached equilibrium in terms of permeate flux rate and transmembrane pressure. An example of a full set of data logged with time is provided in the supplementary information (Supplementary information 2 full run example.csv), and an overview table of the experiments performed is also provided (Supplementary information 3 summary table.csv).

2.4. Suspension characterisation

A 1% w/w suspension of calcite was used, contained in a two litre beaker. The calcite had a surface area to volume (d_{32} or Sauter mean) diameter of 2.7 µm and d05% is approximately 0.7 µm as measured by a Malvern Mastersizer Hydro 2000SM, see Fig. 3. The inset in Fig. 3 shows an SEM image of these solids. The natural pH of the suspension was 8.65 (measured on a calibrated Mettler Toldeo 320 pH meter) and at this pH the Zeta potential has been reported to be −43.7 mV [33]. The cake concentration formed on the microfilter was determined by discharging the cake (after draining) in to weighed dishes and drying to constant mass. A total of 27 gravimetric tests were successfully performed (some tests failed due to cake slippage whilst draining), and the average volume fraction of solids in the cake was determined to be 37% v/v, with a relative standard deviation of 5.4%. Cake depth was measured by photography and a graticule, the precision of the technique providing a measurement to within +/−70 micrometres of the given value. Samples of some cakes were also taken for particle size distribution analysis using the Malvern Mastersizer.

The rheological properties of a compact of the calcite (marginally less than 37% v/v), in water, was tested in a concentric cylinder rheometer (Haake VT550) using the SV-Din geometry at 25 °C. The intention was to measure the rheology of the deposited cake, or a

Table 1
Manufacturer specified properties of the ceramic Coralith C0 microfilter.

Gas filtration nominal pore size (μm)	Liquid filtration nominal pore size (μm)	Average pore diameter (μm)	Maximum pore diameter (μm)	Porosity of filter (%)	Permeability (Darcies)	Strength (Mpa)
0.3	1	11	15	35–45	0.5–1.2	25.5

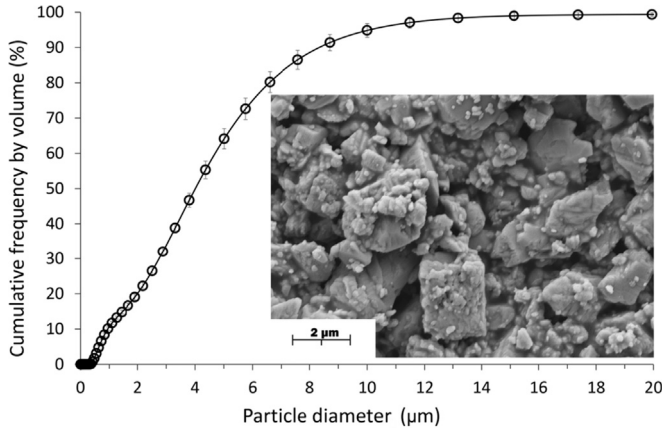

Fig. 3. Particle Size distribution of the calcite used measured by Malvern Mastersizer with SEM inset of particles.

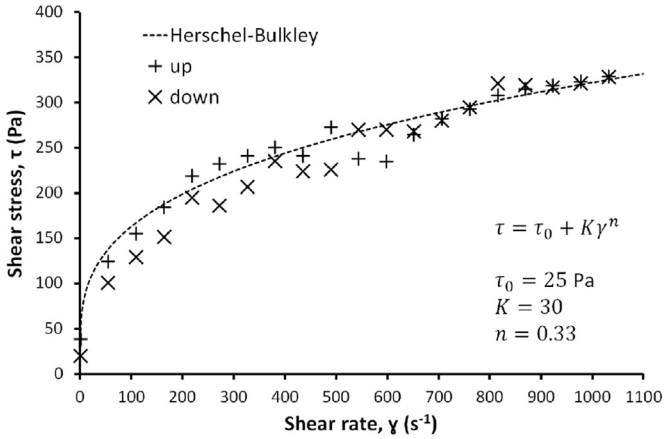

Fig. 4. Rheogram of a 37% v/v calcite slurry, obtained during ascending and descending shear steps and fitted Herschel Bulkley rheological model.

concentration as near to it as practically possible, the compact was transferred to the cup by spatula, after which the rotor was inserted, which displaced the cake to the walls and expelled air from the system. Stepped sweeps increasing and decreasing shear rates across a range of 1–1032 s^{-1}, were performed over a period of 25 min.

3. Results and discussion

In the following discussion it is assumed that shear stress that should be used in the analysis is the 'peak shear' obtained during an oscillation. At any position on the membrane surface the shear will vary, but for the purpose of preventing the deposition of solids it is the peak shear value that will prevent the deposition of material on the surface. To assist in the understanding between the frequency of oscillation employed and the maximum shear stress at the oscillating surface Table 2 provides the correlation between these variables for the ceramic filter, based on a cake thickness of 1.5 mm. This is equivalent to a total radial distance from the centre of oscillation of 16.5 mm, as the clean membrane radial position is 15 mm.

Fig. 4 provides the Herschel-Bulkley rheogram for the compact at a concentration close to that determined to form the filter cake. There appears to be a yield stress of approximately 25 Pa and, once flowing, the suspension exhibits the expected shear thinning behaviour.

Fig. 5 illustrates a typical set of curves for the decay of the permeate flux with respect to time. An equilibrium flux rate of approximately 200 l m^{-2} h^{-1} appears to exist even when filtering in the absence of any shear, in accordance with the K_o component of Eq. (1). The data for oscillation frequencies of 44 and 60 Hz are very similar, but scattered data is common in filtration studies [1] and a yield stress exhibiting material will make this more likely. At higher oscillation frequencies: 80 and 100 Hz, the data is closer to what is expected with consistently increasing equilibrium flux with higher oscillation frequency. Similar

Table 2
Frequency and maximum shear stress values for the ceramic microfilter in azimuthal oscillation – based on a 1.5 mm cake thickness.

Frequency (Hz):	20	40	60	80	100
Maximum shear stress (Pa):	12	44	94	150	225

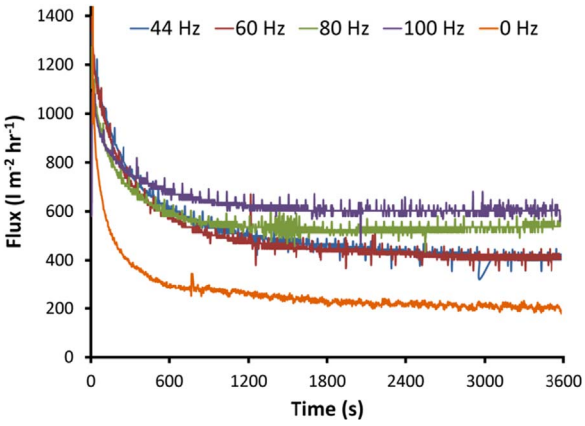

Fig. 5. Permeate flux rate with time for various frequencies of oscillation during filtration using the ceramic membrane in azimuthal mode of shear application.

curves were generated for the different types of filters and the different modes of application of shear. Due to the potential variation in both flux rate and transmembrane pressure the main bulk of results are reported not in terms of flux rate, but in terms of resistance as determined by Eq. (8), based on measurements of instantaneous flux rate and transmembrane pressure.

The ability to frequently record permeate mass and transmembrane pressure enabled an investigation of the initial stages of filtration. It is reasonably well known that these can have a significant influence on the filtration performance, and that the interaction of the suspension and the membrane filter can lead to pore plugging and high values of filter membrane resistance [1], considerably in excess of what would be expected from clean water tests aimed at determining R_m. The changing value of R_m during membrane filtration has been described as one of the most challenging aspects of membrane modelling. This aspect of membrane fouling would be expected to be highly apparent with a system where the membrane pore size is comparable with the particle size to be filtered [34], and when operating at relatively low suspended solids concentration in the feed, as was the case reported here. Fig. 6 shows the apparent total resistance (R_m + R_c) with time at the start of

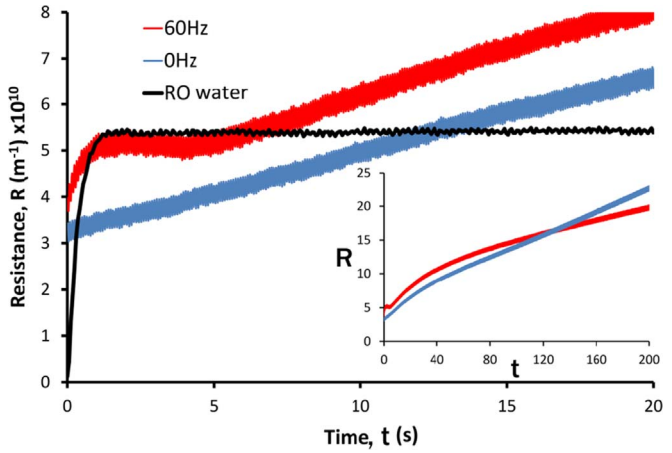

Fig. 6. Apparent total resistance with time near the start of filtration for three conditions; inset shows resistance over 200 s.

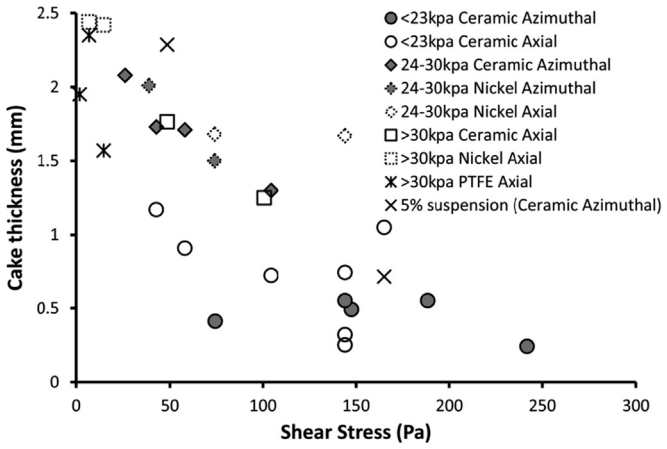

Fig. 7. Filter cake thickness measured after axial and azimuthal oscillation of filter for various filter types, modes of operation and (non-controlled) transmembrane pressures.

the 60 Hz azimuthal oscillation using the ceramic filter. Pore plugging would be expected to be most significant with this type of filter.

There are several items of note visible in Fig. 6. Firstly, the clean (RO) water test appears to provide a stable value of $5.5\times10^{10}\,m^{-1}$. The experiment started with water present in all the flow lines and the filtrate section of the cylindrical filter. Despite all lines being filled with an incompressible fluid the resistance still appears to require 1–2 s to rise up to its equilibrium value. This time was required for the pressure to stabilise, due presumably to some air still being within the circuit close to the pressure transducer surface as well as flexibility of the plastic pipework. However, after 2 s the system stabilised and R_m remained constant. The most surprising result is in comparing the RO water test with the 1% w/w calcite filtration with zero applied shear. In this case the total resistance was less than that measured by the RO water test up to 12 s from the start of the test. The resistance appeared to be rising at constant rate, as would be expected from a constant rate filtration, but the apparent starting resistance was lower than the clean RO water test value. This behaviour occurred for all the ceramic membrane filtrations. It is assumed that in the matrix type of filter pore channels may be opening up. Channels not working (i.e. not taking the flow) will cause a higher flow in the larger diameter channels that do take the flow, leading to a higher measured value of pressure drop and, therefore, resistance. When filtering with no shear some particles may be able to penetrate the filter helping to distribute the flow more evenly within the filter, followed by a cake formation protecting the membrane from further blockage, and flow will be through all the channels within the forming cake. When filtering at 60 Hz behaviour similar to the clean water test is evident, with an initial period (5 s) of total resistance similar to the clean water test. In this case, the shear disrupts cake formation for a short while, after which cake is formed at what looks initially to be the same rate as the zero shear value. The inset graph in Fig. 6 shows that the application of shear does eventually limit the cake depth compared to the zero shear condition, with less overall resistance when applying 60 Hz after about 130 s of filtration.

Based on the observation that a period of constant resistance exists, between 1 and 5 s, and at a value similar to that measured using clean water the value used in the modelling for R_m is $5.5\times10^{10}\,m^{-1}$. This value was found in all the other filtrations using the ceramic filter. Using this value of membrane resistance and the membrane thickness and measured porosity of 37% in Eq. (11) gives an equivalent pore diameter of 1.4 μm, which is close to the nominal value provided by the manufacturer, Table 1. It is highly likely that the membrane will become internally fouled by, at least, some of the particulate material in the challenge suspension. The pore openings on the surface of the filter are significantly larger than most of the challenge suspension, but it is believed that the filter cake will form rapidly, and will protect the filter from further deposition within the 8 mm filter depth. This is supported by the application of Eqs. (12) and (13), after calculating the membrane permeability from Eq.(9) to be $1.45\times10^{-13}\,m^2$, hence using the Kozeny permeability term to give the specific surface to be $4.2\times10^5\,m^2\,m^{-3}$ (i.e. Sauter mean diameter of the particles constituting the original filter to be 14.3 micrometres). Then using the greatest value for pressure drop (32.5 kPa) and fastest flux rate ($1500\,l\,m^{-2}\,h^{-1}$), provides a shear stress within the filter of just under 6 Pa. The yield stress of the calcite compact is 25 Pa (Fig. 4), thus the shear stress within the filter is well below the yield stress of the solid compact at (or just within) the surface layers of the filter. Hence, it is reasonable to conclude that the solid deposit will remain at, or just within, the filter as there is insufficient shear within the filter to drag the deposited cake further in to the filter matrix. This will, therefore, limit the increase in membrane resistance with time.

The measured cake thicknesses are shown in Fig. 7, for all the different types of filter and modes of application of shear. Given the operating conditions permitted some degree of varying transmembrane pressure (obtained by sucking permeate through the system), as well as shear stress, the data has different allocated markers based on the measured transmembrane pressure: less than 23 kPa; 24–30 kPa; and over 30 kPa equilibrium pressures. The maximum transmembrane pressure recorded was 32.5 kPa. In general, high shear gives low cake depth resulting in low pressures, whereas higher pressures were needed to maintain flow through thicker cakes formed at lower shear. The data is scattered, but there is no discernible trend based on the mode of operation of shear (axial or azimuthal), nor does the type of filter appear to influence the resulting cake thickness. Two additional tests were performed to investigate the cake thickness when filtering from a 5% w/w suspension, using ceramic azimuthal conditions. The resulting values were similar to those obtained with the 1% w/w feed suspension, suggesting that the shear plane between the cake adhering to the oscillating filter and the surrounding slurry is close to the cake concentration. The experimental data appears to show that extrapolating to a shear stress of between 250 and 300 Pa would give a cake thickness of zero, the sustainable flux scenario. Eq. (7) could be used to provide an estimate of sustainable flux operation, but more information on the expected sustainable flux rate and the appropriate particle size to use in the equation is required, and will be provided later.

Fig. 8 compares the total resistance at equilibrium during filtration for the different systems. The clean filter membrane resistances are also marked. Again the data is scattered, especially at relatively low values of shear at, or around, what could be near the yield stress. However, again there is no discernible trend for resistance to vary with anything other than shear stress; no noticeable influence of mode of application of shear, nor type of filter. This may be expected of the type of

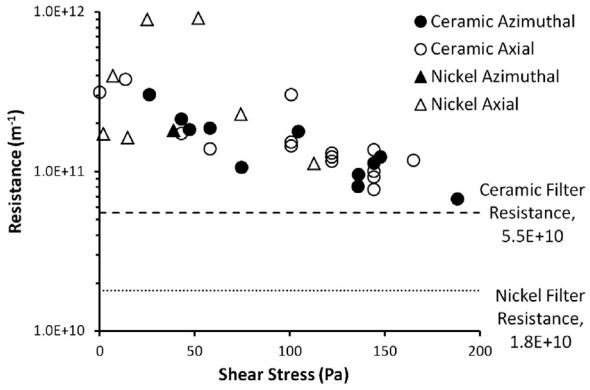

Fig. 8. Total resistance to filtration as a function of shear stress when operating at equilibrium for various filter types and oscillation modes.

microfiltration when a cake, or deposit, is formed on the surface of the membrane. Again extrapolation to a shear condition of between 250 and 300 Pa would suggest a system in which the resistance is determined only by the membrane, i.e. the sustainable flux condition.

Data on the resistance due to the deposited cake and the cake thickness can be used to determine the permeability of the deposit in an analogous way to that shown in Eq. (9) for the membrane. Having determined the deposit permeability it is then possible to calculate the particle size required to give that permeability, using a rearranged form of Eq. (5) and the value of the deposit concentration (37% v/v). This is plotted in Fig. 9, labelled 'Happel and Brenner', together with the measured values of Sauter mean diameter obtained from the cake samples as well as the Sauter mean diameter of the initial material before filtration (2.7 μm). For the experimentally measured values of diameter there is a general trend of a slight reduction in particle size with increasing shear at the membrane surface, as would be expected [1] as the larger particles are more easily removed from (or prevented from depositing on) the membrane surface. However, the measured Sauter mean diameters used in Eq. (5) would give rise to permeabilities that are too great, and resistances too small to match the data contained in Fig. 8. In order to use Eq. (5) to predict the correct permeabilities (and cake resistances) a particle diameter of about 0.74 μm is required – marked by the crosses in Fig. 9. This is approximately equal to the 5% value of the cumulative mass undersize curve (See Fig. 3), as recommended by Wakeman [29]. Thus the representative particle size for the modelling of this system is taken to be 0.74 μm.

Returning to the concept of sustainable flux, using Eq. (3) in Eq. (2) with the particle diameter of 0.74 μm provides a value of $1300\,l\,m^{-2}\,h^{-1}$ ($3.6\times10^{-4}\,m^3\,m^{-2}\,s^{-1}$). Adding the non-shear dependent flux of $200\,l\,m^{-2}\,h^{-1}$ (K_o in Eq.(1)) provides an expected

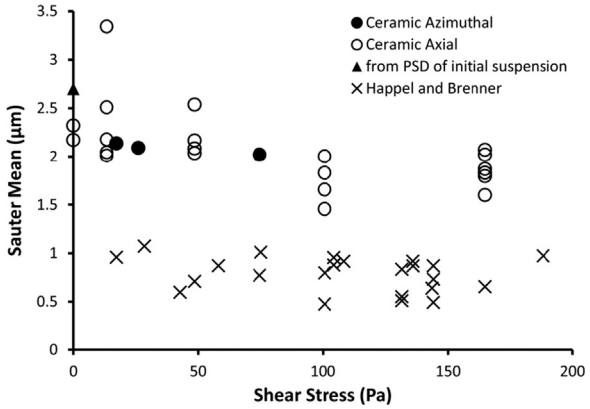

Fig. 9. Measured Sauter mean diameters of filter cakes at different shear stresses by Malvern Mastersizer and, for comparison, deduced particle diameter using measured cake thickness and resistance employing the Happel and Brenner permeability model (Eq. (5)).

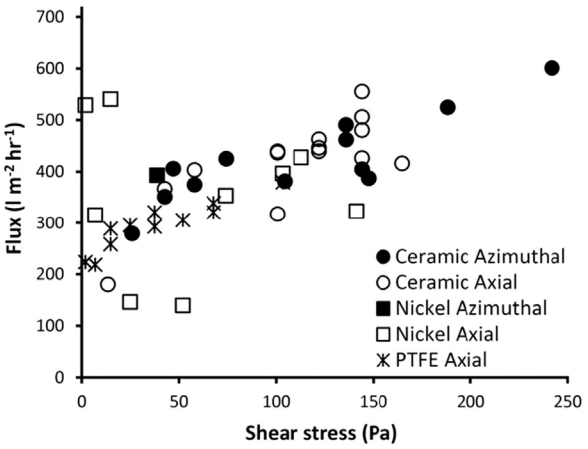

Fig. 10. Permeate flux as a function of shear stress for different applications of shear and type of filters, providing constitutive model (ignoring data below 25 Pa and given in SI units): $J = 4*10^{-7}\tau + 7*10^{-5}$.

sustainable flux of close to $1500\,l\,m^{-2}\,h^{-1}$. It is noticeable that this is in the range of what may be expected if no fouling, or deposit, occurred according to the data at the start of the filtration displayed in Fig. 5.

Fig. 10 shows the data for equilibrium flux as a function of shear stress for the different types of filters and the different modes of application of shear. The data at low shear is very scattered, as may be expected when operating near the yield stress, but again it is possible to conclude that the mode of application of shear and the type of filter (or even filter surface properties) does not influence the flux: it is only a function of the applied shear stress. Regressing a straight line through the data, ignoring the low shear results, provides a gradient of $4\times10^{-7}\,m\,s^{-1}\,Pa^{-1}$. This is the same value calculated when putting Eq. (4) in to Eq. (2), to determine the K_1 component in Eq. (1).

4. Conclusions

Azimuthal oscillation of a microfilter is easily achieved in the laboratory modifying readily available domestic DIY equipment, and at low cost. Comparison of microfiltration performance between azimuthal and axial oscillation showed that the mode of vibration did not influence the filtration performance; equilibrium flux rates for the mineral type of material filtered here are shown to be simply correlated by the peak shear stress delivered by the oscillating system. There was also no influence on the equilibrium flux rate due to the type of filter: slotted surface (hydrophilic metal); slotted surface (PTFE) or a matrix type of ceramic filter. In all cases, the equilibrium flux and cake thickness could be correlated with the shear stress applied to the system. In order to evaluate the shear stress a computational fluid dynamics model was necessary, as the solid concentration at, or close to, the deposited filter cake was sufficiently high that the compact exhibited non-Newtonian behaviour. Similar tests are now being run with even more complex rheological systems, such as iron oxyhydroxide flocs.

The existence of a yield stress in the compact appeared to limit the internal fouling of the matrix type of filter, which had a membrane thickness of 8 mm but, contrary to expectation, did not demonstrate significant internal penetration and fouling of its structure over time, or between filtrations. Tests investigating the initial stages of filtration showed that the measured membrane resistance remained similar to that obtained by classic 'clean water' tests, despite the relatively large pore size and substantial amount of suspended solids material that should have been able to penetrate the filter, if that material behaved as particles capable of being dragged individually into the filter matrix.

A standard approach to the modelling, based on a force balance, appeared to correlate the data well, with realistic values of both the equilibrium flux and the 'sustainable flux' predicted as functions of the

peak shear stress. The permeability of the deposited solids on the filter could also be predicted from a known expression, using the particle size distribution data and the deposit concentration. However, the most appropriate particle diameter to characterise the material was found to be the D05; i.e. the particle size at which 5% of the distribution lies below. This is very significantly lower than the often used D50, the median particle size, or D3,2 the Sauter mean diameter. However, this result is consistent with what has been recommended before, by others, for conventional (dead-end) filtration.

The membrane-type independent results indicate that the main resistance dominating the equilibrium flux in these tests is due to the deposit, and not an interaction of membrane surface and suspended solids. Thus, a high value of sustainable flux would require very high shear, to minimise the deposit thickness. Oscillation of the filter is an appropriate method to achieve this, as the reversal of direction leads to higher values of shear than simply rotating the filter, due to the inertia of the fluid which takes a finite time to reverse direction during which the filter is moving in the opposite direction to the fluid. All the filters described here had varying shear at their surface, but unlike a disc based oscillating filter, the magnitude of shear was identical at all positions on the filter surface at any instant in time. Whereas shear on a disc based system is high at the disc periphery, and minimal towards the centre of the disc. Scaling to a larger surface area filtration system using parallel filters would be simple for axial oscillation, where a spring-based resonant plate can be used to attach filters that axially oscillate. However, scaling an azimuthal oscillating system would be more complex.

Acknowledgement

The authors wish to express their gratitude to Sellafield Ltd. who sponsored the work through the DISTINCTIVE collaboration, with the EPSRC Grant Ref: EP/L014041/1.

Appendix A. Supplementary material

Supplementary material associated with this article can be found in the online version at http://dx.doi.org/10.1016/j.memsci.2017.12.079.

References

[1] G. Foley, Membrane Filtration a Problem Solving Approach with MATLAB, Cambridge University Press, Cambridge, UK, 2013.
[2] E.P. Byrne, J.J. Fitzpatrick, L.W. Pampel, N.J. Titchener-Hooker, Influence of shear on particle size and fractal dimension of whey protein precipitates: implications for scale-up and centrifugal clarification efficiency, Chem. Eng. Sci. 57 (2002) 3767–3779.
[3] M.Y. Jaffrin, L.-H. Ding, O. Akoum, A. Brou, A hydrodynamic comparison between rotating disk and vibratory dynamic filtration systems, J. Membr. Sci. 242 (2004) 155–167.
[4] F. Zamani, J.W. Chew, E. Akhondi, W.B. Krantz, A.G. Fane, Unsteady-state shear strategies to enhance mass-transfer for the implementation of ultrapermeable membranes in reverse osmosis: a review, Desalination 356 (2015) 328–348.
[5] D. Herman, M. Poirier, M. Fowley, M. Keefer, T. Huff, Testing of the second generation Spintek rotary filter, in: Proceedings of Conference: WM Management Symposia, Department of Energy, Phoenix, AZ, USA, 27 Feb- 3 March 2011.
[6] L.-H. Ding, M.Y. Jaffrin, M. Mellal, G. He, Investigation of performances of a multishaft disk (MSD) system with overlapping ceramic membranes in microfiltration of mineral suspensions, J. Membr. Sci. 276 (2006) 232–240.
[7] G. He, L.-H. Ding, P. Paullier, M.Y. Jaffrin, Experimental study of a dynamic filtration system with overlapping ceramic membranes and non-permeating disks rotating at independent speeds, J. Membr. Sci. 300 (2007) 63–70.
[8] Z. Tu, L. Ding, Microfiltration of mineral suspensions using a MSD module with rotating ceramic and polymeric membranes, Sep. Purif. Technol. 73 (2010) 363–370.
[9] L. Liu, X. Xu, C. Zhao, F. Yang, A new helical membrane module for increasing permeate flux, J. Membr. Sci. 360 (2010) 142–148.
[10] L. Jie, L. Liu, F. Yang, F. Liu, Z. Liu, The configuration and application of helical membrane modules in MBR, J. Membr. Sci. 392–393 (2012) 112–121.
[11] T. Jiang, H. Zhang, F. Yang, D. Gao, H. Du, Relationships between mechanically induced hydrodynamics and membrane fouling in a novel rotating membrane bioreactor, Desalin. Water Treat. 51 (2013) 2850–2861.
[12] M.R. Bilad, G. Mezohegyi, P. Declerck, I.F.J. Vankelecom, Novel magnetically induced membrane vibration (MMV) for fouling control in membrane bioreactors, Water Res. 46 (2012) 63–72.
[13] T. Li, A.W.-K. Law, M. Cetin, A.G. Fane, Fouling control of submerged hollow fibre membranes by vibrations, J. Membr. Sci. 427 (2013) 230–239.
[14] G. Genkin, T. Waite, A.G. Fane, S. Chang, The effect of vibration and coagulant addition on the filtration performance of submerged hollow fibre membranes, J. Membr. Sci. 281 (2006) 726–734.
[15] M.Y. Jaffrin, Dynamic shear-enhanced membrane filtration: a review of rotating disks, rotating membranes and vibrating systems, J. Membr. Sci. 324 (2008) 7–25.
[16] H.G. Gomaa, S. Rao, M.A. Taweel, Flux enhancement using oscillatory motion and turbulence promoters, J. Membr. Sci. 381 (2011) 64–73.
[17] O. Akoum, M.Y. Jaffrin, L. Ding, P. Paullier, C. Vanhoutte, An hydrodynamic investigation of microfiltration and ultrafiltration in a vibrating membrane module, J. Membr. Sci. 197 (2002) 37–52.
[18] S. Beier, M. Guerra, A. Garde, G. Jonsson, Dynamic microfiltration with a vibrating hollow fiber membrane module: filtration of yeast suspensions, J. Membr. Sci. 281 (2006) 281–287.
[19] F. Zhao, H. Chu, Y. Zhang, S. Jiang, Z. Yu, X. Zhou, Increasing the vibration frequency to mitigate reversible and irreversible membrane fouling using an axial vibration membrane in microalgae harvesting, J. Membr. Sci. 529 (2017) 215–223.
[20] M.T. Stillwell, W. Sumritwatchasai, R.G. Holdich, S. Kosvintsev, Low pressure microfilter design aspects and filtration performance, Sep. Sci. Technol. 44 (2009) 2541–2558.
[21] Z. Jalilvand, F.Z. Ashtiani, A. Fouladitajar, H. Rezaei, Computational fluid dynamics modelling and experimental study of continuous and pulsatile flow in flat sheet microfiltration membranes, J. Membr. Sci. 450 (2014) 207–214.
[22] M.D. Petala, A.I. Zouboulis, Vibratory shear enhanced processing membrane filtration applied for the removal of natural organic matter from surface waters, J. Membr. Sci. 269 (2006) 1–14.
[23] H.G. Gomaa, S. Rao, A.M. Al-Taweel, Intensification of membrane microfiltration using oscillatory motion, Sep. Purif. Technol. 78 (2011) 336–344.
[24] J. Postlethwaite, S.R. Lamping, G.C. Leach, M.F. Hurwitz, G.J. Lye, Flux and transmission characteristics of a vibrating microfiltration system operated at high biomass loading, J. Membr. Sci. 228 (2004) 89–101.
[25] O. Akoum, M.Y. Jaffrin, L.-H. Ding, Concentration of total milk proteins by high shear ultrafiltration in a vibrating membrane module, J. Membr. Sci. 247 (2005) 211–220.
[26] N.J. Blake, I.W. Cumming, M. Streat, Prediction of steady state crossflow filtration using a force balance model, J. Membr. Sci. 68 (1992) 205–215.
[27] J.D. Sherwood, The force on a sphere pulled away from a permeable half-space, Physiochem. Hydrodyn. 10 (1998) 3–12.
[28] Happel, Brenner, Low Reynolds number hydrodynamics, Kluwer Boston, Inc., Hingham, USA, 1983.
[29] R. Wakeman, The influence of particle properties on filtration, Sep. Purif. Technol. 58 (2007) 234–241.
[30] P. Bacchin, P. Aimar, R. Field, Critical and sustainable fluxes: theory, experiments and applications, J. Membr. Sci. 281 (2006) 42–69.
[31] R.G. Holdich, Fundamentals of Particle Technology, Midland Information Technology, Shepshed, UK, 2002.
[32] T.C. Papanastasiou, Flow of materials with yield, J. Rheol. 31 (1987) 385–404.
[33] P. Moulin, H. Roques, Zeta potential measurement of calcium carbonate, J. Colloid Interface Sci. 261 (2003) 115–126.
[34] A. Rushton, A.S. Ward, R.G. Holdich, Solid-Liquid Filtration and Separation Technologies, Wiley-VCH, Weinheim, Germany, 1996.